Optimal estimation in polarimetric imaging in the presence of correlated noise fluctuations

Julien Fade, Swapnesh Panigrahi, Mehdi Alouini

Optimal estimation in polarimetric imaging in the presence of correlated noise fluctuations

Julien Fade,* **Swapnesh Panigrahi, and Mehdi Alouini**

Institut de Physique de Rennes, Université de Rennes 1, CNRS, Campus de Beaulieu, 35042 Rennes, France

*julien.fade@univ-rennes1.fr

Abstract: We quantitatively analyze how a polarization-sensitive imager can overcome the precision of a standard intensity camera when estimating a parameter on a polarized source over an intense background. We show that the gain is maximized when the two polarimetric channels are perturbed with significantly correlated noise fluctuations. An optimal estimator is derived and compared to standard intensity and polarimetric estimators.

OCIS codes: (110.5405) Polarimetric imaging; (110.4280) Noise in imaging systems; (110.3055) Information theoretical analysis; (030.6600) Statistical optics; (110.0113) Imaging through turbid media.

References and links

1. M. P. Rowe, J. S. Tyo, N. Engheta, and E. N. Pugh, "Polarization-difference imaging: a biologically inspired techniquefor observation through scattering media," Opt. Lett. **20**, 608–610 (1995).
2. S. Demos, H. Savage, A. S. Heerdt, S. Schantz, and R. Alfano, "Time resolved degree of polarization for human breast tissue," Opt. Commun. **124**, 439–442 (1996).
3. O. Emile, F. Bretenaker, and A. L. Floch, "Rotating polarization imaging in turbid media," Opt. Lett. **21**, 1706–1708 (1996).
4. H. Ramachandran and A. Narayanan, "Two-dimensional imaging through turbid media using a continuous wave light source," Opt. Commun. **154**, 255–260 (1998).
5. J. Guan and J. Zhu, "Target detection in turbid medium using polarization-based range-gated technology," Opt. Express **21**, 14152–14158 (2013).
6. G. D. Lewis, D. L. Jordan, and P. J. Roberts, "Backscattering target detection in a turbid medium by polarization discrimination," Appl. Opt. **38**, 3937–3944 (1999).
7. P. Réfrégier, M. Roche, and F. Goudail, "Cramer-Rao lower bound for the estimation of the degree of polarization in active coherent imagery at low photon levels," Opt. Lett. **31**, 3565–3567 (2006).
8. A. Bénière, F. Goudail, M. Alouini, and D. Dolfi, "Degree of polarization estimation in the presence of nonuniform illumination and additive gaussian noise," J. Opt. Soc. Am. A **25**, 919–929 (2008).
9. M. Boffety, F. Galland, and A.-G. Allais, "Influence of polarization filtering on image registration precision in underwater conditions," Opt. Lett. **37**, 3273–3275 (2012).
10. M. Dubreuil, P. Delrot, I. Leonard, A. Alfalou, C. Brosseau, and A. Dogariu, "Exploring underwater target detection by imaging polarimetry and correlation techniques," Appl. Opt. **52**, 997–1005 (2013).
11. A. Bénière, M. Alouini, F. Goudail, and D. Dolfi, "Design and experimental validation of a snapshot polarization contrast imager," Appl. Opt. **48**, 5764–5773 (2009).
12. N. Hautiere and D. Aubert, "Contrast restoration of foggy images through use of an onboard camera," in *Proceedings of 2005 IEEE Intelligent Transportation Systems* (2005), pp 601–606.
13. N. Gracias, S. Negahdaripour, L. Neumann, R. Prados, and R. Garcia, "A motion compensated filtering approach to remove sunlight flicker in shallow water images," in *OCEANS 2008*, (2008), pp. 1–7.
14. M. Darecki, D. Stramski, and M. Sokólski, "Measurements of high-frequency light fluctuations induced by sea surface waves with an underwater porcupine radiometer system," J. Geophys. Res. **116**, C00H09 (2011).
15. F. A. Sadjadi and C. L. Chun, "Automatic detection of small objects from their infrared state-of-polarization vectors," Opt. Lett. **28**, 531–533 (2003).

#200923 - $15.00 USD Received 8 Nov 2013; revised 22 Dec 2013; accepted 23 Dec 2013; published 24 Feb 2014

16. B. Laude-Boulesteix, A. D. Martino, B. Drévillon, and L. Schwartz, "Mueller polarimetric imaging system with liquid crystals," Appl. Opt. **43**, 2824–2832 (2004).
17. J. Jaffe, "Computer modeling and the design of optimal underwater imaging systems," IEEE J. Oceanic Eng. **15**, 101–111 (1990).
18. P. Garthwaite, I. Jolliffe, and B. Jones, *Statistical Inference* (Prentice Hall, 1995).
19. J. Fade, N. Treps, C. Fabre, and P. Réfrégier, "Optimal precision of parameter estimation in images with local sub-Poissonian quantum fluctuations," Eur. Phys. J. D **50**, 215–227 (2008).

1. Introduction and posing of the problem

1.1. Introduction

Polarimetric-sensitive detectors (PSD) have long been implemented and have proved efficient in many application fields, such as biomedical imaging [1, 2], and vision/contrast enhancement through turbid media [3–5]. In this context, the benefits of polarimetric imaging have been thoroughly investigated by considering various imaging architectures and noise models [6–9]. However, the gain in measurement precision that can be reached when a PSD is used instead of a standard intensity detector (ID), in the presence of significantly correlated noise fluctuations in each polarimetric channel, is still unexplored to the best of our knowledge. Indeed, for practical reasons it is usually assumed that these noise fluctuations are uncorrelated. As a result, considering the most favorable situation of a perfectly polarized source (or polarizing object) embedded in unpolarized background, the polarimetric channel which offers the best contrast is the one corresponding to the polarization state of the source. In this channel, the mean intensity level of the source is thus preserved, whereas that of the unpolarized background is reduced by a factor of two, leading to a doubling of contrast as compared to standard intensity detection [1, 10]. Nevertheless, the assumption of uncorrelated noise fluctuations is not representative of most real field scenarios especially when the polarimetric channels are acquired simultaneously [11]. For instance, a polarized source appearing through fog or haze is a situation where the background mean level is time-varying [12] especially when the imaging system is moving or vibrating. More generally, similar situations might be encountered when imaging objects through turbid media, as in the fields of underwater imaging [13, 14], or infrared target detection [15]. Imaging a static scene might also be subject to intensity fluctuations of the illuminating source, as often encountered in polarimetric microscopy [16]. Thus, one can wonder whether the noise correlation properties of the different polarimetric channels could be properly exploited in order to optimize, in terms of contrast, the representation of the polarimetric image.

In this article, we intend to rigorously quantify the gain in measurement precision that can be reached when a PSD is used in the presence of significantly correlated noise fluctuations in each polarimetric channel. This article is organized as follows: in the remainder of the first Section, we describe the general polarimetric image formation model addressed, as well as the correlated-noise statistical model considered throughout this article. Within the theoretical framework of information theory, the benefit of using PSD instead of a standard ID is then derived in Section 2, for a general estimation problem consisting in measuring a parameter (intensity, absorbance, location, etc.) on a polarized source over an intense background. The expression of this gain in optimal estimation precision is then thoroughly analyzed in Section 3 in relation with realistic experimental imaging conditions. Lastly, optimal estimation procedures are derived and discussed in Section 4, before providing conclusions of the article in Section 5.

#200923 - $15.00 USD Received 8 Nov 2013; revised 22 Dec 2013; accepted 23 Dec 2013; published 24 Feb 2014

1.2. Image formation model

We will consider a general framework consisting in the estimation of a given parameter (intensity, location, etc.) from a polarized signal contribution, denoted s_i at location i, with a degree of polarization (DOP) denoted by $P \in [0,1]$, which is either emitted by an active source or backscattered by an object of interest. Using a simple classical but realistic illumination model [9, 10, 17], the intensity X_i^I detected at location i is assumed to also comprise a background contribution b_i, with a DOP denoted by $\beta \in [0,1]$. This background contribution is due to ambient light scattering through a turbid medium (atmosphere, water, or biological tissue). For the sake of generality, we shall analyze any couple of polarization parameters P and β which can correspond to many different experimental conditions. Although in most experiments the signal contribution is highly polarized in comparison to an unpolarized background ($P \gg \beta$), some situations can involve opposite physical conditions ($\beta \gg P$), such as underwater imaging as mentioned in [10].

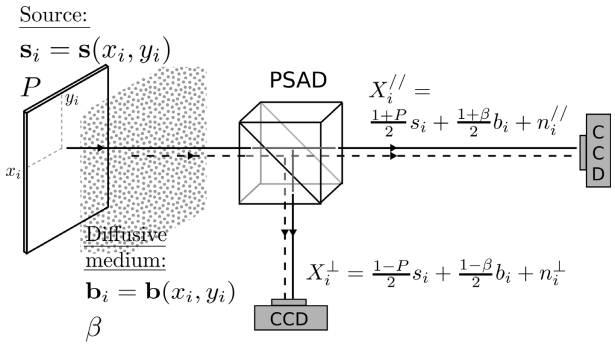

Fig. 1. Sketch of the image formation model: a polarization-splitting analyzing device (PSAD) can be any suitable birefringent crystal in case of simultaneous acquisitions of images $\mathbf{X}^{//}$ and $\mathbf{X}^{\perp}$ [11], or a rotating polarizer or liquid crystal device for sequential acquisitions. Image formation optics are not represented for the sake of clarity.

A non-polarimetric ID with N pixels gives access to a sample $\mathbf{X}_i^I = \{X_i^I\}_{i=1,\ldots,N}$, with $\langle X_i^I \rangle = s_i + b_i$, whereas a PSD provides a bidimensional vector $\mathbf{X}_i^P = \left[X_i^{//},\ X_i^{\perp}\right]^T$ at each location i of the detector, obtained from the intensities recorded along two orthogonal polarization directions [11], as sketched in Fig. 1. With the above illumination model, the average value of $\mathbf{X}_i^P$ is simply given by

$$\langle \mathbf{X}_i^P \rangle = \begin{bmatrix} \frac{1+P}{2} s_i + \frac{1+\beta}{2} b_i \\ \frac{1-P}{2} s_i + \frac{1-\beta}{2} b_i \end{bmatrix}. \tag{1}$$

1.3. Noise model

Throughout this article, we shall consider a Gaussian noise model, which makes it possible to take into account various sources of noise in realistic situations. In addition, such model provides closed-form expressions which is in favour of physical interpretation. At a given location i, the second order statistical properties of the bidimensional measurement vector $\mathbf{X}_i^P$ are modeled by a covariance matrix $\Gamma_i = \left\langle \delta\mathbf{X}_i^P \left(\delta\mathbf{X}_i^P\right)^T \right\rangle$, with $\delta\mathbf{X}_i^P = \mathbf{X}_i^P - \langle \mathbf{X}_i^P \rangle$, of the following form:

$$\Gamma_i = \begin{bmatrix} \sigma_{//,i}^2 & c_i \\ c_i & \sigma_{\perp,i}^2 \end{bmatrix} = \begin{bmatrix} \frac{1+\beta}{2}\varepsilon_i^2 + \sigma_0^2 & \rho\frac{\sqrt{1-\beta^2}}{2}\varepsilon_i^2 \\ \rho\frac{\sqrt{1-\beta^2}}{2}\varepsilon_i^2 & \frac{1-\beta}{2}\varepsilon_i^2 + \sigma_0^2 \end{bmatrix}.$$

#200923 - $15.00 USD Received 8 Nov 2013; revised 22 Dec 2013; accepted 23 Dec 2013; published 24 Feb 2014

The Gaussian probability density function of a $N-$pixels measurement sample is then given by $P_{\mathbf{X}}(\mathbf{X}^P) = \prod_{i=1}^{N} \exp\{-\frac{1}{2}\left(\delta\mathbf{X}_i^P\right)^T \Gamma_i^{-1} \delta\mathbf{X}_i^P\}/2\pi\sqrt{\det[\Gamma_i]}$.

Table 1. List and description of symbols and acronyms. Dependency in scene location *i* has been omitted for the sake of concision.

Symbols:		**Acronyms:**	
s / b	Source / background mean value	PSD	Polarization-sensitive detector
P / β	Source / background DOP		
$\mathbf{X}^I$ / $\mathbf{X}^P$	Intensity / polarimetric sample measured	ID	Intensity detector
$X^{//}$ / $X^{\perp}$	Orthogonal polarimetric measures	DOP	Degree of polarization
Γ	Covariance matrix of $\mathbf{X}^P$	PSAD	Polarization-splitting analyzing device
$\sigma_{//}^2$ / $\sigma_{\perp}^2$	Noise variance on polarimetric channels		
σ_0^2	Detector electronic noise variance	FI / I_F	Fisher information
ε^2	Optical multiplicative noise variance	CRB	Cramer-Rao bound
ω^2	Ratio of noise variances ($\omega^2 = \varepsilon^2/\sigma_0^2$)	SNR	Signal-to-noise ratio
ρ	Correlation parameter	ML	Maximum likelihood
μ / μ_∞	Gain / asymptotic gain in optimal estimation precision		
$\hat{s}_{ML}^I$ / $\hat{s}_{ML}^P$	Intensity / polarimetric ML estimator		
$\hat{s}_{\Delta}^P$	Polarimetric difference estimator		

Let us focus on the parallel channel: through this statistical description, we assume that the noise variance can be written $\sigma_{//,i}^2 = (1+\beta)\varepsilon_i^2/2 + \sigma_0^2$, with the detector electronic noise contribution σ_0^2 being rationally independent from the location i in the image, and from the illumination level or polarization properties. The first term in the expression of $\sigma_{//,i}^2$ accounts for a multiplicative "optical" noise, introduced by background optical intensity fluctuations, and hence depends on the background DOP β. This noise contribution, proportional to the background average level b_i, can model the effect of turbulence or variations of scatterers density, as well as photon noise in the high background intensity limit.

Due to these scene-dependent optical fluctuations, the intensity measurements in the two polarimetric channels are likely to be correlated, especially in the case of simultaneous acquisition of the polarimetric images with a polarization-splitting analyzing device (PSAD), as sketched in Fig. 1 or as extensively described in [11]. Such partial correlation will be modeled by a non-null covariance term c_i in Γ_i. We assume that the scene-dependent noise contributions only are partially correlated through a correlation parameter ρ, whereas the detector noise is assumed to be uncorrelated between the two channels.

2. Gain in optimal estimation performance

2.1. Principle

To characterize the gain in terms of estimation precision when PSDs are used instead of classical IDs, we propose to resort to information theory, by determining and comparing the Fisher Information (FI) associated to each imaging modality. The FI characterizes the amount of information available in a sample $\mathbf{X}$ for the estimation of a parameter y, and is defined as [18]

$$\mathrm{I_F}(y) = -\left\langle \frac{\partial^2 \ln P_{\mathbf{X}}(\mathbf{X})}{\partial y^2} \right\rangle. \tag{2}$$

According to the well-known Cramer-Rao theorem, its inverse value $\mathrm{I_F}^{-1}(y)$ defines a lower bound (Cramer-Rao bound (CRB)) on the minimum variance expectable for estimating param-

#200923 - $15.00 USD Received 8 Nov 2013; revised 22 Dec 2013; accepted 23 Dec 2013; published 24 Feb 2014

eter y with an unbiased estimation procedure [18]. In the following, we shall limit ourselves to the estimation of the mean signal intensity s_i at location i for the sake of simplicity but without loss of generality. Indeed, it is possible to extrapolate the results of this article to other physical situations since one has $\mathrm{I_F}(z) = \mathrm{I_F}(y)\left[dy/dz\right]^2$ from simple variable transformation relations. For instance, for the estimation of an atmospheric transmittance τ such that $s = e^{-L\tau}$, the FI is directly obtained with $\mathrm{I_F}(\tau) = L^2 s^2 \mathrm{I_F}(s)$, which simply involves the FI for the estimation of the mean signal intensity $\mathrm{I_F}(s)$. Another illutration is the interesting case of image registration addressed in [9], in which a translation parameter η is to be estimated over the whole image such that $\mathbf{s} = \{s(x_i - \eta)\}_{i=1,\ldots,N}$. In this latter case, the above relation yields $\mathrm{I_F}(\eta) = \sum_{i=1}^{N} [s'(x_i - \eta)]^2 \mathrm{I_F}(s_i)$, which again only involves the FI for the estimation of the mean intensity at each location i.

2.2. *Expression of the gain*

The FI in the case of polarimetric and intensity measurements are derived in Appendix A, and are not recalled here for the sake of concision. We propose to define a gain in optimal precision by comparing the FI available with a polarimetric setup over the FI available with a standard intensity detector, for given experimental conditions. This definition, which has been used in other references [9, 19], yields:

$$\mu(\omega, P, \beta, \rho) = \frac{\mathrm{I_F}^P(s)}{\mathrm{I_F}^I(s)} = \frac{(1+\omega^2)\left[\frac{1+P^2}{2} + \frac{Q}{4}\omega^2\right]}{1 + \omega^2 + \frac{(1-\rho^2)(1-\beta^2)}{4}\omega^4}, \tag{3}$$

where

$$Q = (1 - 2\beta P + P^2) - \rho(1 - P^2)\sqrt{1-\beta^2}, \tag{4}$$

and with $\omega^2 = \varepsilon^2/\sigma_0^2$. This last parameter ω^2 gives the relative value of the noise contributions variances, allowing one to identify the dominant noise term. Thus, "optical" noise ε^2 dominates when $\omega^2 \gg 1$, whereas electronic fluctuations are the main source of noise when $\omega^2 \ll 1$. As an illustration, the evolution of the gain $\mu(\omega, P, \beta, \rho)$ given in Eq. (3) is plotted in Fig. 2 as a function of ρ for various values of ω, and for a partially polarized source ($P = 0.4$) and background ($\beta = 0.1$). It can be immediately checked that the gain does not depend on ρ when electronic noise dominates ($\omega \ll 1$), and that it increases as ω increases.

As will be shown in the following, such definition of a gain in optimal estimation precision can provide insightful results on the physical estimation problem at hands, regardless of the actual estimation procedure used, since derived from information theory. In addition, it can have practical implications if optimal estimators can be identified, as will be shown in Section 4.

3. Physical analysis of the gain $\mu(\omega, P, \beta, \rho)$

In this section, we derive and analyze a number of properties of the gain in optimal precision $\mu(\omega, P, \beta, \rho)$ defined above. These results will allow us to study the benefits of using PSDs for estimation tasks in the presence of intense background and potentially correlated measurements.

3.1. *Influence of ambient illumination level*

Let us first study how the gain evolves as a function of the ambient background illumination level b. For that purpose, we analyze the behaviour of the gain $\mu(\omega, P, \beta, \rho)$ as a function of $\omega = \varepsilon/\sigma_0$, since ε has been assumed proportional to b. A tractable but tedious calculus sketched in Appendix B leads to this first property:

#200923 - $15.00 USD Received 8 Nov 2013; revised 22 Dec 2013; accepted 23 Dec 2013; published 24 Feb 2014

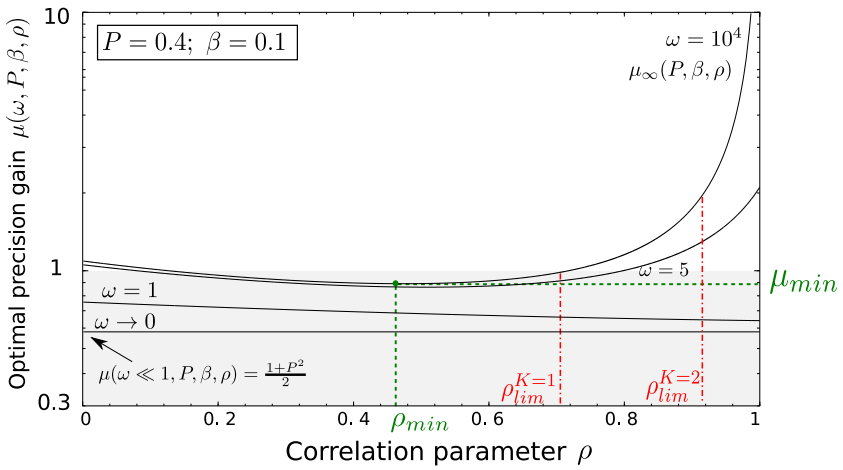

Fig. 2. Evolution of $\mu(\omega,P,\beta,\rho)$ for $P = 0.4$ and $\beta = 0.1$ as a function of ρ for $\omega = \{10^{-3},1,5,10^4\}$.

Property 1 *The gain $\mu(\omega,P,\beta,\rho)$ is a monotonically increasing function of ω.*

This is an interesting result, showing that increasing the relative amount of "optical" noise with respect to electronic noise tends to favour a polarimetric setup in terms of estimation performance, even if the polarimetric measurements are totally uncorrelated ($\rho \to 0$).

When electronic noise dominates, the gain falls down below unity, since $\mu(\omega \ll 1,P,\beta,\rho) \to (1+P^2)/2 \leq 1$. Indeed, for a given amount of light energy entering the imaging system, the PSAD reduces the signal-to-noise ratio (SNR) on the detectors in comparison to a standard ID since energy is splitted into two polarization channels. This property can be checked in Fig. 2 where $\mu(\omega,P,\beta,\rho)$ is plotted as a function of ρ, when $P = 0.4$ and $\beta = 0.1$.

3.2. Asymptotic behaviour in the high intensity regime

Focusing on the high intensity regime by setting $\omega \to \infty$, we obtain a simpler expression

$$\mu_\infty(P,\beta,\rho) = \mu(\omega \gg 1,P,\beta,\rho) = \frac{Q}{(1-\rho^2)(1-\beta^2)}, \tag{5}$$

which will be referred to as *asymptotic gain* subsequently.

Let us analyze the evolution of the asymptotic gain as a function of the correlation between polarimetric channels. Surprisingly, it can be shown that $\mu_\infty(P,\beta,\rho)$ is not a monotonically increasing function of the correlation parameter ρ, as can be observed in Fig. 2. The following property can indeed be demonstrated (see Appendix C):

Property 2 *The asymptotic gain $\mu_\infty(P,\beta,\rho)$ reaches a minimum value $\mu_{\infty,min}$ for a correlation parameter ρ_{min}, such that*

$$\begin{cases} \mu_{\infty,min} = \frac{(1+P)^2}{2(1+\beta)} & \text{and} \quad \rho_{min} = \frac{1-P}{1+P}\sqrt{\frac{1+\beta}{1-\beta}}, \quad \text{if} \quad \beta \leq \frac{2P}{1+P^2} \\ \mu_{\infty,min} = \frac{(1-P)^2}{2(1-\beta)} & \text{and} \quad \rho_{min} = \frac{1+P}{1-P}\sqrt{\frac{1-\beta}{1+\beta}}, \quad \text{otherwise} \end{cases} \tag{6}$$

This property is rather counter-intuitive but can be interpreted as follows. First, when the two acquired polarimetric images are uncorrelated ($\rho \simeq 0$), gain in estimation precision only occurs

#200923 - $15.00 USD Received 8 Nov 2013; revised 22 Dec 2013; accepted 23 Dec 2013; published 24 Feb 2014

if SNR reduction caused by intensity splitting between the two polarization channels is compensated by the increase in size of the statistical sample considered (Two sets of N measures with a PSD, instead of one in an standard ID). Though, as soon as $\rho \neq 0$, the polarimetric measures are no longer independent, and thus the available FI is necessarily lower than the one available with two independent sets of N measurements. This remains true for smaller values of ρ. However, for values of $\rho > \rho_{min}$, the strongly correlated noise perturbing each polarization channel can be partly cancelled out by taking profit of the two acquired images, leading to a potentially strong increase in the gain. This is indeed possible if signal and background contributions exhibit different relative intensity levels on the two acquired images. In this case, an optimal estimation procedure, such as the one described in Section 4, can take profit of this relative contrast mismatch to estimate the desired parameter on the signal contribution with a high precision.

Using the expression of the asymptotic gain given in Eq. (5), let us now analyze in which physical conditions one should favour using a PSD rather than a standard ID. For that purpose, the two following properties can be established. A sketch of the demonstration of these properties is given in Appendix D.

Property 3 *For a given value of P, the asymptotic gain $\mu_\infty(P,\beta,\rho)$ is greater or equal to a minimum gain value K (with $K \geq 1$) for any value of the correlation parameter ρ provided*

$$\beta \leq \frac{(1+P)^2}{2K} - 1, \quad \textit{if} \quad \beta \leq P, \tag{7}$$

$$\beta \geq 1 - \frac{(1-P)^2}{2K} \quad \textit{if} \quad \beta \geq P. \tag{8}$$

Property 4 *When the conditions of Property 3 are not verified, the asymptotic gain $\mu_\infty(P,\beta,\rho)$ is greater or equal to a minimum gain value K (with $K \geq 1$) provided the correlation parameter ρ verifies*

$$\rho \geq \rho_{lim}^K = \frac{1-P^2}{2K\sqrt{1-\beta^2}} + \sqrt{\Phi}, \tag{9}$$

where

$$\Phi = \left[1 - \frac{1}{2K}\frac{(1-P)^2}{1-\beta}\right] \times \left[1 - \frac{1}{2K}\frac{(1+P)^2}{1+\beta}\right]. \tag{10}$$

3.3. Discussion

The previous properties provide conditions on the physical parameters at hand in order to ensure a minimum gain K when using PSDs instead of standard imagers. In this subsection, we propose to quantitatively analyze these theoretical results.

We obviously start focusing on the case of unitary gain (i.e., $K = 1$) which delimitates situations in which polarimetric imaging systems can bring an improvement in estimation precision. In this case, the conditions of Eqs. (7) and (8) respectively read $\beta \leq (1+P)^2/2 - 1$ when $\beta \leq P$, and $\beta \geq 1 - (1-P)^2/2$ when $\beta \geq P$. For a fully depolarized background ($\beta = 0$), for instance, this means that a polarimetric imaging system can improve the quality of estimation, whatever be the value of ρ, as long as a moderately polarized source is used with a minimum value of $P = \sqrt{2} - 1 \simeq 0.414$. On the other hand, when the source is totally unpolarized, a gain can be expected for any value of ρ provided $\beta \geq 1/2$. In the two-dimensional plot of Fig. 3(a) as a function of polarization parameters P and β, the conditions of Eqs. (7) and (8) for $K = 1$ are represented with continuous green curves and delimitate two regions. When the conditions hold (greyed region in Fig. 3(a)), the values of $\mu_{\infty,min}$ and ρ_{min} are represented in contour plots,

#200923 - $15.00 USD Received 8 Nov 2013; revised 22 Dec 2013; accepted 23 Dec 2013; published 24 Feb 2014

respectively in blue dashed lines and green dot-dashed lines. In the second region, i.e., when the inequalities of Eqs. (7) and (8) are not verified, the correlation parameter ρ has to be greater than a minimum value denoted $\rho_{lim}^{K=1}$ so as to ensure $\mu_\infty(P,\beta,\rho) \geq 1$. The values of $\rho_{lim}^{K=1}$ are plotted in Fig. 3(a) in red continuous lines, as a function of P and β.

The same graphical representation has been used in Fig. 3(b)-3(d) in the case of $K = \{2,5,10\}$ respectively, to plot the values of ρ_{min} and $\mu_{\infty,min}$ when the relation of Eq. (8) holds, and the values of ρ_{lim}^{K} otherwise. It is interesting to notice that when $P \geq \beta$, a limit value $\rho_{lim}^{K} > 0$ always has to be ensured for any couple of parameters P and β as long as $K \geq 2$ since condition of Eq. (7) cannot be fulfilled in this case. On the other hand, when a highly polarized background is considered and $\beta \geq P$, a high asymptotic gain value K can be reached with uncorrelated measurements (i.e., $\rho = 0$) provided P is small enough. This property can be understood by noticing that a high value of β implies a low background contribution on one of the two acquired images, thus facilitating estimation of a parameter on the low polarized signal contribution. This result must be however mitigated since the detector noise has been neglected to derive Properties 3 and 4, but should be taken into account in this latter case involving low background illumination levels.

In terms of practical application, the charts given in Fig. 3 provide insightful information about the expectable gain in precision using a PSD for a given set of physical parameters P, β and ρ. As could be expected, the best performance gain is obtained when a high polarimetric contrast can be observed between the background and signal contributions (high P and low β, or high β and low P). However, these charts clearly evidence that the gain in performance increases also when the measurements are significantly correlated. Yet, these charts may be of great use to assess the optimal performance of a real field polarimetric imaging system, in which all intermediate situations are likely to occur. For instance, the degradation of the DOP of a highly polarized source could be taken into account in the dimensioning of an experiment. The influence of unwanted or unexpected polarization/depolarization of the background could be also analyzed with the above results.

4. Optimal estimation procedure

The relevance of the above results is however conditioned to the definition of *efficient* estimation procedures, i.e., estimators ensuring unbiased estimation and a minimum variance which reaches the CRB studied above. Let us thus consider estimators of s in the maximum likelihood (ML) sense, since ML estimators are known to be *efficient* under Gaussian fluctuations [18], which is the noise model considered throughout this article. Limiting ourselves to the high intensity regime ($\omega \to \infty$), and assuming that the background mean value b is *a priori* known, the ML estimator of s using a standard intensity detector is simply given by $\hat{s}_{ML}^{I} = \hat{X}^{I} - b$. When a polarimetric imager is used, the derivation of the ML estimator of s is detailed in Appendix E and leads to

$$\hat{s}_{ML}^{P} = \frac{U\hat{X}^{//} + V\hat{X}^{\perp} + Z}{W}, \tag{11}$$

where U, V, W and Z are functions of P, β, ρ and b, which parameters are assumed *a priori* known. These functions can be easily derived from Appendix E with appropriate changes of variable, but are not detailed here for brevity reasons. Both ML estimators are unbiased, i.e., $\langle \hat{s}_{ML}^{P} \rangle = \langle \hat{s}_{ML}^{I} \rangle = s$, and their variances are easily compared using the above characterization of the FIs since they respectively reach the CRBs computed above in the cases of polarimetric and intensity measurements. As a result, the gain studied in the previous section corresponds to the ratio of the variances of these two ML estimators: $\mu_\infty(P,\beta,\rho) = \mathrm{var}(\hat{s}_{ML}^{I})/\mathrm{var}(\hat{s}_{ML}^{P})$.

For a fair comparison, the estimation samples should involve the same number of pixels. Thus, a PSD with N pixels in each polarimetric channels must be compared to a $2N$-pixels

#200923 - $15.00 USD Received 8 Nov 2013; revised 22 Dec 2013; accepted 23 Dec 2013; published 24 Feb 2014

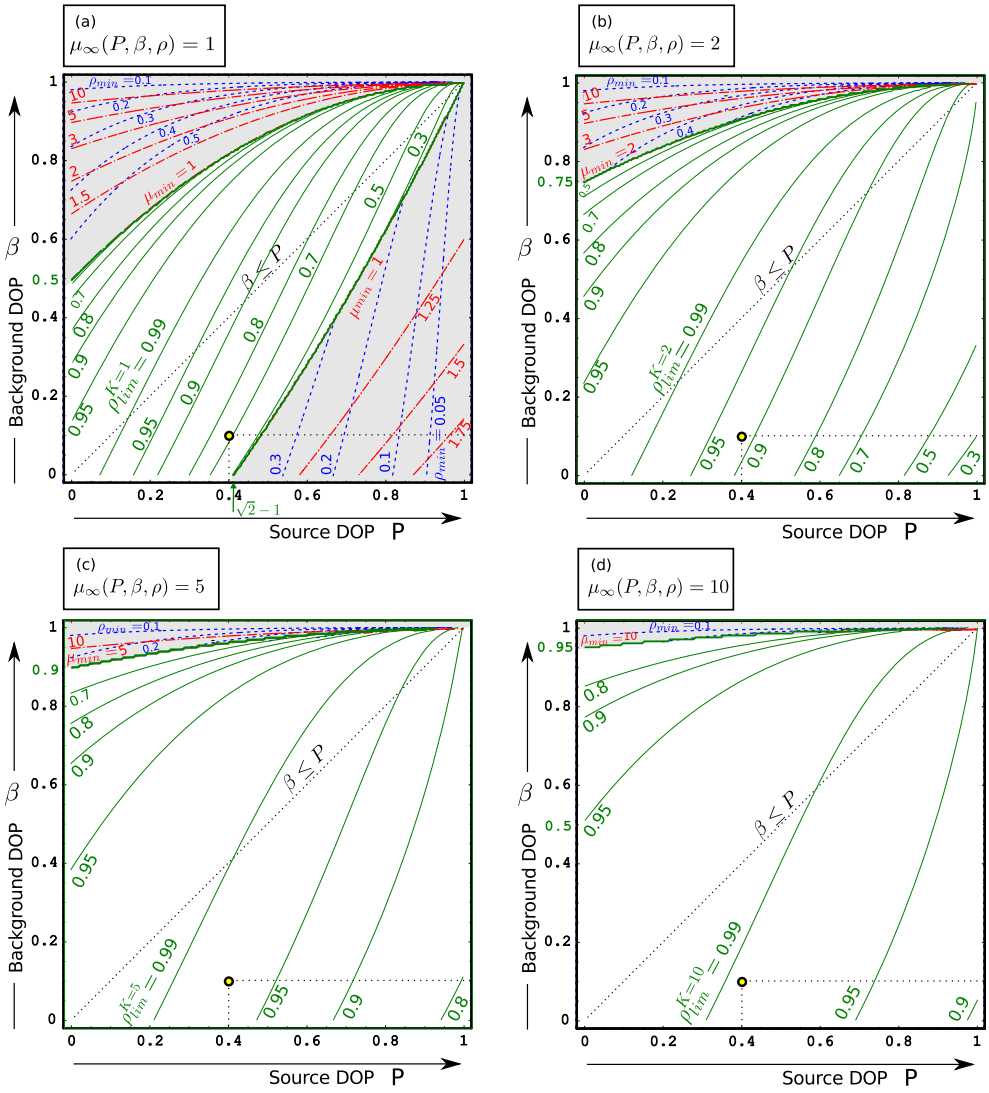

Fig. 3. Contour plots of ρ_{lim}^{K} for various values of K as a function of P and β. Additional contour plots of ρ_{min} and $\mu_{\infty,min}$ are provided when relations (7) and (8) hold. The yellow circles correspond to the situation addressed in Fig. 2 ($P=0.4$ and $\beta=0.1$).

standard ID. In this case, the relative performance of the two estimators can be directly assessed from the chart plotted in Fig. 3(b), which gives conditions for a minimum gain value of $\mu_\infty(P,\beta,\rho)\geq K=2$. The analyzis of this chart interestingly shows that PSDs are not systematically preferable to standard ID if the correlation between the fluctuations lies below a lower limit $\rho_{lim}^{K=2}$ determined above. As a result, the chart plotted in Fig. 3(b) turns out to be a useful tool for determining the optimal estimation procedure, depending on the experimental conditions.

Lastly, it can be interesting to compare the ML estimator with other estimation procedures which are classically used in polarimetric imaging. For instance, when polarimetric measure-

#200923 - $15.00 USD Received 8 Nov 2013; revised 22 Dec 2013; accepted 23 Dec 2013; published 24 Feb 2014

ments along orthogonal polarization directions are available, a simple *difference* image is classically obtained by substraction of the two polarimetric channels [1]. For the estimation of the parameter s, such *difference* estimator would simply read $\hat{s}_{\Delta}^{P} = [\hat{X}^{//} - \hat{X}^{\perp} - \beta b]/P$. However, it can be shown that this standard estimator is not optimal, in general, in the situation addressed in this article. Its variance, derived in Appendix F, is indeed greater that $\mathrm{var}(\hat{s}_{ML}^{P})$ (and thus greater than the CRB) except when $\rho = (1-\beta P)/(1-\beta^2)$, in which case the difference estimator $\hat{s}_{\Delta}^{P}$ identifies with $\hat{s}_{ML}^{P}$.

5. Conclusion

As a conclusion, the theoretical results derived in this article quantitatively demonstrate that polarimetric imagers can significantly improve the estimation precision, provided noise fluctuations in each polarimetric channels are significantly correlated. Hence, this confirms the interest of snapshot polarimetric imagers as described in [11] since they may favour correlated background/noise fluctuations in the two polarimetric channels, which are acquired simultaneously. In these conditions, we have also shown that the optimal estimation procedure differs from a natural *difference* image, but can be simply implemented. These results can be useful for the design of polarimetric imaging systems involving estimation through turbid media, or in other fields of application, for post-processing of polarimetric images exhibiting temporally or spatially correlated fluctuations.

Appendix

To derive the expressions presented in this article, it is interesting to introduce the following simplified notations: $a = (1+P)/2$ and $\alpha = (1-P)/(1+P)$ on the one hand, and, on the other hand, $c^2 = (1+\beta)/2$ and $\gamma^2 = (1-\beta)/(1+\beta)$. In a single pixel configuration ($N = 1$) for the sake of simplicity, the polarimetric measurement considered is $\mathbf{X}^P = [X^{//},\ X^{\perp}]^T$, such that $\langle \mathbf{X}^P \rangle = [as + c^2 b,\ \alpha as + \gamma^2 c^2 b]^T$ and

$$\Gamma = \langle \delta\mathbf{X} \delta\mathbf{X}^T \rangle = c^2 \begin{bmatrix} \varepsilon^2 + \varsigma^2 & \rho\gamma\varepsilon^2 \\ \rho\gamma\varepsilon^2 & \gamma^2\varepsilon^2 + \varsigma^2 \end{bmatrix},$$

with $\varsigma^2 = 2\sigma_0^2/(1+\beta)$. It is easily checked that the conditions $P \in [0,1]$, $\beta \in [0,1]$ and $\beta \leq P$ are equivalent to $\alpha \in [0,1]$, $\gamma \in [0,1]$ and $\gamma^2 \geq \alpha$.

A. Fisher informations calculations

With the Gaussian noise model used in this article, the loglikelihood of the polarimetric measure $\mathbf{X}^P$ can be written $\ell(\mathbf{X}^P) = \ln P_{\mathbf{X}}(\mathbf{X}^P) = -\left(\delta\mathbf{X}^P\right)^T \Gamma^{-1} \delta\mathbf{X}^P/2$ up to an additive term independent of s. An application of Eq. (2) leads to the FI for the estimation of s, which reads $\mathrm{I_F}^P(s) = \left[\langle \mathbf{X} \rangle'^P\right]^T \Gamma^{-1} \langle \mathbf{X} \rangle'^P$, with $\langle \mathbf{X} \rangle'^P = \partial \langle \mathbf{X} \rangle^P / \partial s = \langle \partial \mathbf{X}^P / \partial s \rangle = [a,\ a\,\alpha]^T$. A direct calculation gives:

$$\mathrm{I_F}^P(s) = \frac{a^2}{c^2\varepsilon^2} \cdot \frac{(\alpha^2 - 2\rho\alpha\gamma + \gamma^2) + (1+\alpha^2)u^{-2}}{\gamma^2(1-\rho^2) + (1+\gamma^2)u^{-2} + u^{-4}}, \tag{12}$$

with $u^2 = \varepsilon^2/\varsigma^2 = (1+\beta)\,\omega^2/2$.

The FI for the estimation of s from the total intensity of the beam (non-polarimetric measurement) is a standard result under Gaussian fluctuations hypothesis. One has

$$\mathrm{I_F}^I(s) = \frac{a^2}{c^2\varepsilon^2} \cdot \frac{(1+\alpha)^2}{(1+\gamma^2) + u^{-2}} = \frac{\sigma^{-2}}{1+\omega^2}. \tag{13}$$

#200923 - $15.00 USD Received 8 Nov 2013; revised 22 Dec 2013; accepted 23 Dec 2013; published 24 Feb 2014

The gain $\mu(u,\alpha,\gamma,\rho) = \mathrm{I_F}^P(s)/\mathrm{I_F}^I(s)$ can then be easily derived, leading to Eq. (3) with appropriate changes of variables.

B. Monotonicity of $\mu(u,\alpha,\gamma,\rho)$ as a function of u

To demonstrate Property 1, let us first rewrite $\mu(u,\alpha,\gamma,\rho)$ as

$$\mu(u,\alpha,\gamma,\rho) = \frac{Au^2+B}{Du^4+Cu^2+1} \times \frac{Cu^2+1}{E}, \tag{14}$$

with $A=(\alpha^2-2\rho\alpha\gamma+\gamma^2)$, $B=1+\alpha^2$, $C=1+\gamma^2$, $D=\gamma^2(1-\rho^2)$ and $E=(1+\alpha)^2$, all these expressions being greater or equal to zero. Let us notice that $\mu(0,\alpha,\gamma,\rho)=B/E=(1+P^2)/2$.

The derivative of $\mu(u,\alpha,\gamma,\rho)$ as a function of u is thus

$$\frac{\partial[\mu(u,\alpha,\gamma,\rho)]}{\partial u} = \frac{2u\mathscr{H}(u)}{\left[1+Cu^2+Du^4\right]^2 E}, \tag{15}$$

with $\mathscr{H}(u) = A+2(AC-BD)u^2+(AC^2-AD-BCD)u^4$.

The function $\mu(u,\alpha,\gamma,\rho)$ is monotonically increasing on $u\in[0;\infty[$ if $\partial[\mu(u,\alpha,\gamma,\rho)]/\partial u \geq 0 \Leftrightarrow \mathscr{H}(u)\geq 0,\ \forall u\in[0;\infty[$. Noticing that $\mathscr{H}(0)=A\geq 0$, and that $\mathscr{H}(u)$ is a second-order polynomial in u^2, we can compute the discriminant

$$\Delta = 4D(A^2+DB^2-ABC) = -4\gamma^2(1-\rho^2)\left[\alpha(1-\gamma^2)-\rho\gamma(1-\alpha^2)\right]^2, \tag{16}$$

which is negative. As a consequence, $\mathscr{H}(u)$ does not admit real root on $u\in[0;\infty[$, and hence, $\mathscr{H}(u)$ is positive on $u\in[0;\infty[$. As a result, $\mu(u,\alpha,\gamma,\rho)$ is a positive, monotonically increasing function of u for $u\in[0;\infty[$.

C. Minimum value of the asymptotic gain $\mu_\infty(\alpha,\gamma,\rho)$:

The asymptotic gain is obtained by setting $u\to\infty$:

$$\mu_\infty(\alpha,\gamma,\rho) = \frac{(\alpha^2-2\rho\alpha\gamma+\gamma^2)(1+\gamma^2)}{\gamma^2(1-\rho^2)(1+\alpha)^2} \tag{17}$$

It is easily shown that $\mu_\infty(\alpha,\gamma,\rho)$ reaches a minimum if $(\alpha\rho-\gamma)(\alpha-\rho\gamma)=0$. Since $\rho\in[0,1]$, the only admissible root is $\rho_{min}=\alpha/\gamma$ when $\gamma\geq\alpha$ and thus $\mu_{\infty,min}(\alpha,\gamma)=(1+\gamma^2)/(1+\alpha)^2$. When $\gamma\leq\alpha$, the only admissible root is $\rho_{min}=\gamma/\alpha$, and in this case $\mu_{\infty,min}(\alpha,\gamma)=\alpha^2(1+\gamma^2)/\gamma^2(1+\alpha)^2$. The expressions of ρ_{min} and $\mu_{\infty,min}(P,\beta)$ given in the article can be recovered with an appropriate change of variables.

From the above results, the conditions for $\mu_{\infty,min}(\alpha,\gamma)\geq K$ are directly derived as

$$\gamma^2 \geq K(1+\alpha)^2-1 \quad \text{when} \quad \gamma\geq\alpha \tag{18}$$

$$\gamma^2 \leq \alpha^2/\left[K(1+\alpha)^2-\alpha^2\right] \quad \text{when} \quad \gamma\leq\alpha. \tag{19}$$

D. Condition for minimum gain $\mu_\infty(\alpha,\gamma,\rho)=K$:

Solving $\mu_\infty(\alpha,\gamma,\rho)=K$ leads to two roots $\rho^K_{1/2}=\left[\alpha(1+\gamma^2)\mp\sqrt{\Phi}\right]/K\gamma(1+\alpha)^2$ verifying $\rho^K_{1/2}\in[0,1]$, with $\Phi=\left[1+\gamma^2-K(1+\alpha)^2\right]\left[\alpha^2(1+\gamma^2)-K(1+\alpha)^2\gamma^2\right]$, or with the notations of Appendix B, $\Phi=\left[C-KE\right]\left[\alpha^2C-KE\gamma^2\right]$.

Let us focus on the greatest root, denoted $\rho^K_{lim}=\rho^K_2$ in the following, and which defines the minimum value of ρ such that $\mu_\infty(\alpha,\gamma,\rho)\geq K,\ \forall\rho\geq\rho^K_{lim}$. It can first be checked that

#200923 - $15.00 USD Received 8 Nov 2013; revised 22 Dec 2013; accepted 23 Dec 2013; published 24 Feb 2014

the expressions of ρ_{lim}^K and Φ respectively given in the Eqs. (9) and (10) of Property 4 can be retrieved with appropriate changes of variables. In particular, one has $\Phi = \Psi/\left[K^2\gamma^2(1+\alpha)^4\right]$.

Let us now study in which conditions this upper root ρ_{lim}^K actually defines a real-valued limit on the correlation parameter ρ. It is clear that ρ_{lim}^K is imaginary if $\Phi \leq 0$, which occurs when one of the two following inequalities is verified: (a): $\alpha^2 C/\gamma^2 E \leq K \leq C/E$; or (b): $\alpha^2 C/\gamma^2 E \geq K \geq C/E$. When $\gamma \geq \alpha$, inequality (b) is impossible, and (a) is verified if $\gamma^2 \geq K(1+\alpha)^2 - 1$. When $\gamma \leq \alpha$, inequality (a) is impossible, and (b) is verified if $\gamma^2 \leq \alpha^2/\left[K(1+\alpha)^2 - \alpha^2\right]$. These conditions obviously correspond to those derived above in Appendix C in Eqs. (18) and (19) for ensuring $\mu_{\infty,min}(\alpha,\gamma) \geq K$.

For the sake of physical interpretation, we can rewrite these conditions as

$$\gamma^2 \geq K(1+\alpha)^2 - 1, \quad \text{if} \quad \alpha \leq \gamma^2, \quad \text{and} \tag{20}$$

$$\gamma^2 \leq \alpha^2/\left[K(1+\alpha)^2 - \alpha^2\right], \quad \text{if} \quad \alpha \geq \gamma^2, \tag{21}$$

which allows relations (7) and (8) of Property 3 to be retrieved by appropriate change of variables. Indeed, it can be checked that none of the conditions of Eqs. (18) and (19) apply when $\gamma^2 \leq \alpha \leq \gamma$.

E. ML estimator $\hat{s}_{ML}^P$

We derive the ML estimator in a situation of negligible detector noise, i.e., $u \to \infty$ (or $\omega \to \infty$). From the expression of $\ell(\mathbf{X}^P)$ given in Appendix A, we derive $\hat{s}_{ML}^P$ by solving $\partial\ell(\mathbf{X}^P)/\partial s = 0$, leading to equation $\left(\delta\mathbf{X}^P\right)^T\Gamma^{-1}\langle\mathbf{X}\rangle' + \left(\langle\mathbf{X}\rangle'\right)^T\Gamma^{-1}\delta\mathbf{X}^P = 0$. A straightforward but tedious calculation finally gives the expression of Eq. (11), with $U = \gamma[\gamma - \alpha\rho]$, $V = [\alpha - \gamma\rho]$, $Z = bc^2\gamma[\rho(\alpha+\gamma^2) - \gamma(1+\alpha)]$, and $W = a[\alpha^2 - 2\rho\alpha\gamma + \gamma^2]$. It is easily checked that this estimator is unbiased $\langle\hat{s}_{ML}^P\rangle = s$, since $\langle\hat{X}^{//}\rangle = as + c^2 b$ and $\langle\hat{X}^{\perp}\rangle = a\alpha s + c^2\gamma^2 b$. Moreover, the variance of this estimator necessarily reaches the CRB since ML estimator is efficient under Gaussian fluctuations [18]. This can be checked by noticing that $\mathrm{var}(\hat{s}_{ML}^P) = \left[U^2\,\mathrm{var}(\hat{X}^{//}) + V^2\,\mathrm{var}(\hat{X}^{\perp}) + UV\,\mathrm{cov}(\hat{X}^{//},\hat{X}^{\perp})\right]/W^2$ which, after a simplification step, is equal to $\lim_{u\to\infty}\{1/\mathrm{I_F}^P(s)\}$.

F. Difference image estimator $\hat{s}_{\Delta}^P$

With the notations used in this appendix, the estimator $\hat{s}_{\Delta}^P$ given in Section 4 reads $\hat{s}_{\Delta}^P = \left[(\hat{X}^{//} - \hat{X}^{\perp}) - bc^2(1-\gamma^2)\right]/\left[a(1+\alpha^2)\right]$. One easily checks that it is unbiased and that $\mathrm{var}(\hat{s}_{\Delta}^P) = \left[\mathrm{var}(\hat{X}^{//}) + \mathrm{var}(\hat{X}^{\perp}) - 2\mathrm{cov}(\hat{X}^{//},\hat{X}^{\perp})\right]/\left[a^2(1+\alpha)^2\right]$, which is equal to $\mathrm{var}(\hat{s}_{\Delta}) = c^2\varepsilon^2\left[1+\gamma^2-2\rho\gamma\right]/\left[a^2(1+\alpha)^2\right]$.

Lastly, it can be shown that $\mathrm{var}(\hat{s}_{\Delta}^P) = \mathrm{var}(\hat{s}_{ML}^P)$ if $\alpha + \gamma^2 - \rho(1+\alpha)\gamma = 0$, i.e., if $\rho = (\alpha+\gamma^2)/\gamma(1+\alpha) = (1-\beta P)/(1-\beta^2)$, in which case $\hat{s}_{\Delta}^P = \hat{s}_{ML}^P$.

Acknowledgments

This work has been supported by the TDF company and by Rennes Metropole through Dr. J. Fade's *AIS* grant.

#200923 - $15.00 USD Received 8 Nov 2013; revised 22 Dec 2013; accepted 23 Dec 2013; published 24 Feb 2014